ELSEVIER

Thermochimica Acta 279 (1996) 205–213

thermochimica acta

Thermal reduction of $AlVMoO_7$

I.L. Botto*, M.B. Vassallo

Química Inorgánica, QUINOR, Facultad de Ciencias Exactas, Universidad Nacional de La Plata, CC. 962, La Plata (1900), Argentina

Received 6 July 1995; accepted 20 December 1995

Abstract

The TPR (temperature programmed reduction) study of the $AlVMoO_7$ phase, belonging to the Al_2O_3–V_2O_5–MoO_3 system, has been carried out by means of X-ray diffraction analysis, IR spectroscopy and SEM scanning electron microscopy (including EPMA analysis). The reduction behavior of V_2O_5 and MoO_3 monometallic oxides is included for comparison.

Keywords: Mo–V–Al system; Oxidation/catalyst; TPR

1. Introduction

New phases in the M_2O_3–V_2O_5–MoO_3 system (M is Al, Fe, Cr) have recently been studied [1–6]. Some of them are interesting because of their wide range of potential applications in the catalysis field.

It is well known that MoO_3 and V_2O_5 have catalytic activity and selectivity towards a large number of oxidation reactions [7]. Another metallic species is usually employed to promote this activity [8]. This type of catalytic system is, in general, supported on Al_2O_3 or SiO_2.

The reducibility of the monometallic oxides has been extensively studied [9, 10]. It has been found that the reduction reaction of transition metal oxides to lower oxides and metallic phases is usually a two-step or multistep process. But the reactivity of the metallic element is highly affected when it is part of a mixed oxide, in which a cooperative catalytic effect is then expected.

In order to analyze the chemical nature and reactivity of some compounds of this system, the temperature programmed reduction of the $FeVMoO_7$ phase has recently

* Corresponding author.

SSDI 0040-6031(96)02849-3

been reported [11]. The synthesis and some properties of $Cr_{1-x}Fe_xVMoO_7$ solid solutions have also recently been analyzed [12]. Application of the TPR technique to the $AlVMoO_7$ phase is described in this paper. Study of the thermal behavior of this phase is particularly interesting in the field of catalysis because the activity of the Mo and V species can be affected by their interaction with the Al_2O_3 support.

In general, oxidic catalysts consist of a monolayer of an Mo or V compound on the carrier, although it has also been suggested that multilayers could be formed. However, when the transition metal contents are high, the formation of binary oxides, such as aluminum molybdate or vanadate, is observed. Hence, the active-phase concentration influences the relative amount and type of the new species formed on the support surface [13].

The $AlVMoO_7$ TPR results are compared and discussed with others of related phases, with the aid of X-ray diffraction, IR spectroscopy and SEM scanning electron microscopy (including EPMA).

2. Experimental

The $AlVMoO_7$ phase was obtained by a solid state reaction using V_2O_5, MoO_3 (from the thermal decomposition of ammonium heptamolybdate) and $Al_2O(CH_3COO)_4$ as starting materials. Heating was done in several steps (air atmosphere): 450°C (24 h); 500°C (24 h); 650°C (72 h) and 700°C (24 h). The presence of a single phase was checked by XRD analysis and electron microprobe.

The TPR measurements were carried out in a reactor fed with 10% H_2 (as reducing agent) in an N_2 stream. The temperature was raised up to 1100°C at a heating rate of 10°C min^{-1}. The hydrogen consumed was detected by a thermal conductivity cell.

The XRD analyses were performed in a Phillips PW 1714 diffractometer with Cu Kα radiation and an Ni filter. The quantitative analysis was performed using NaCl as an external standard. Cell parameters were refined by means of the PIRUM program of Werner [14].

The IR spectra were recorded with a Perkin-Elmer 580-B spectrometer using the KBr pellet technique.

The scanning electron microscopical characterization was carried out in a Phillips 505 instrument, with an EDAX 9100 accessory.

3. Results and discussion

Fig. 1 shows the TPR profile of the $AlVMoO_7$ phase. A weak peak is observed at 502°C, while the most intense signals are located at 586 and 955°C respectively.

The TPR pattern of the $FeVMoO_7$ related phase showed two strong peaks at 704 and 1008°C. The first was associated with the formation of MoO_2 and FeV_2O_4 spinel phases, whereas the second was attributed to the formation of Mo metal [11]. The presence of $FeMoO_4$ was also detected in a first stage of the reduction.

Unlike the iron(III) compound, in $AlVMoO_7$ the stability of the trivalent aluminum plays a determining role in the reduction process. Consequently, a different behavior

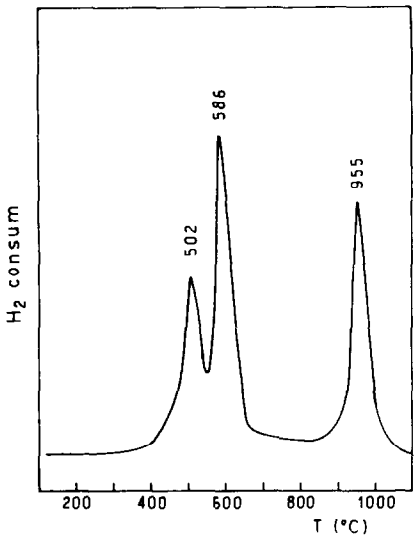

Fig. 1. TPR pattern of the $AlVMoO_7$ phase.

must be expected. Comparison between the MoO_3 and V_2O_5 TPR patterns as bulk and Al_2O_3-supported materials shows differences related to the interaction between compound and support. Experimental parameters such as the concentration of the supported species, hydrogen concentration, total flow rate, heating rate, amount of samples, preconditioning of the sample, etc., also have significant influence on the appearance of the TPR profiles [13,15]. Comparison among results obtained for a particular sample measured under different conditions is very difficult due to these factors. However, the ranges of the reduction temperatures for bulk and γ-Al_2O_3-supported V and Mo monometallic oxides reported in the literature [10,13,15], are summarized in Fig. 2.

Under our experimental conditions, the bulk MoO_3 pattern shows a weak peak at $\approx 500°C$ associated with Mo_4O_{11} formation, although an incipient reduction to MoO_2 is also observed at this temperature. However, the main region in which the Mo(VI)→Mo(IV) process takes place is between 600 and 800°C [16] (730°C in this work). The further Mo(IV)→Mo reduction, which usually occurs between 840 and 910°C [10–18], is observed here at 852°C.

However, the first peak of reduction for MoO_3/Al_2O_3 appears at a lower temperature (between 400 and 600°C), while the second is also shifted to lower values in relation to that observed for MoO_3 bulk ($\approx 800°C$). The area ratio of MoO_3 signals depends on the Mo content and is related to the degree of metallic dispersion (mono or multilayer). The $Al_2(MoO_4)_3$ TPR profile has also been reported, presenting a unique peak at $\approx 530°C$ [13,19].

For bulk V_2O_5 the TPR patterns show a series of discrete peaks, located between 600 and 750°C, associated with a stepwise $V_2O_5 \rightarrow V_2O_3$ reduction, through intermediates that include V_5O_{19} and VO_2 [10,16,20]. Supported on Al_2O_3, the V_2O_5 TPR patterns

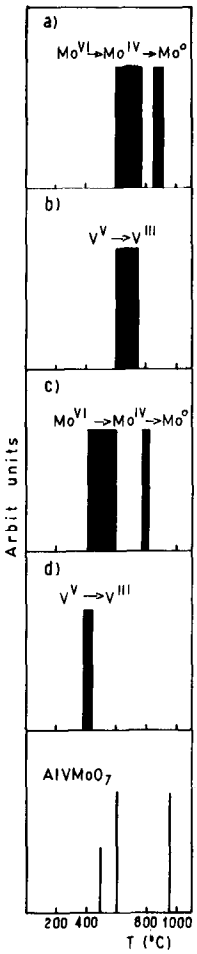

Fig. 2. Comparative TPR patterns showing the main temperature regions of reduction for: a, MoO_3 (bulk); b, V_2O_5 (bulk); c, MoO_3 supported on γ-Al_2O_3; d, V_2O_5 supported on γ-Al_2O_3; e, studied compound.

show, in general, a single signal at $\approx 400°C$, depending on the experimental characteristics. In addition, the reduction profile was found to be significantly dependant on the morphology of the V_2O_5 [20], but it is clear that the reduction stoichiometry always leads to V_2O_3 formation [21]. The mechanism of V_2O_5 reduction by H_2 depends on several factors such as the surface concentration of the capping oxygen, the structural characteristics of the oxide phase on the support and the surface amorphousness in the bulk phase, etc. [22].

In multimetallic oxides, the reduction reaction is a very complex process in which new oxidic phases are formed through several steps. In our recent study of the reducibility of some heteropolyoxomolybdates containing Fe, Al and Co [17], a particular behavior of the Al-phase has been found. In fact, the reduction temperature of

the $[AlMo_6O_{24}H_6]^{3-}$ Anderson-type heteropolyanion to form Mo(IV) occurs at a temperature 100°C lower than that corresponding to the MoO_3, whereas the further reduction to Mo^0 occurs at a temperature $\approx$ 100°C higher than that observed in the MoO_3. This behavior was associated with the formation of the non-stoichiometric $(Al,Mo)O_2$ phase, related to "reduced rutile" [17]. In fact, it can be assumed that the non-stoichiometry is accommodated by CS planes and also by "additional" interstitial small trivalent atoms (and not by a deficit in the O-array) [17,23]. As in the case of the Anderson phase, the "MoO_2" cell volume obtained by the $AlVMoO_7$ reduction becomes slightly larger (by approx. 7‰) than MoO_2 (PC-PDF No. 32-671). It is interesting to comment that for dioxides stucturally related to rutile, there is a close relation between the c/a axial ratio and the metal–metal distance [24,25]. In general, it is observed that the cell volume increases whereas both the axial ratio and the metal–metal length decrease [24]). Monoclinic MoO_2, belonging to a highly distorted rutile structure, shows an equivalence between $(c/a)_{rutile}$ and $d/\sqrt{bc\,\mathrm{sen}\,\beta}$ (where d denotes the length of the metal–metal bonds which extend approximately parallel to the a-axis of the unit cell [24]. Its short metal–metal distance is similar to that observed in the metallic phase. Contrarily, the cell volume is higher than that of other related phases such as VO_2, TiO_2, and others where Mo(IV) has been partially substituted by species with ionic radii < 0.65 Å [23,25,26]. Hence, the formation of an "MoO_2" phase with "instertitial" Al(III) can be suggested as being responsible for a higher metal–metal length which, finally, affects the temperature of its reduction to Mo.

A comparative analysis of the X-ray diffraction patterns of the stages of reduction, in a limited region between 20° and 41° of 2θ, is shown in Fig. 3. Fig. 3a presents the typical lines of the $AlVMoO_7$ phase, which remain unchanged up to 450°C. However, at $\approx$ 500°C (Fig. 3b), their intensities decrease while the most intense lines of $Al_2(MoO_4)_3$ are incipient. Figs. 3c and d show the patterns of the samples heated up to 600 and 1050°C respectively. The PC-PDF of V_2O_3 (No. 34-187), MoO_2 (No. 32-671), $Al_2(MoO_4)_3$ (No. 23-764), δ-Al_2O_3 (No. 16-394) and Mo (No. 42-1120) are included for comparative purposes. It is observed that V(V) reduces to V(III) forming rhombohedral V_2O_3 (isostructural with α-Al_2O_3). The formation of intermediates of vanadium has not been detected by XRD. The VO_2 phase (PC-PDF No. 19-1401) obtained by reducing Al-doped vanadium oxide should be assumed at 500°C, on the basis of the intensity of the lines around 28° 2θ (where the two most intense diffraction lines appear: 27.42° and 28.30°). In contrast, the presence of $Al_2(MoO_4)_3$ has been clearly revealed. This last compound, as well as MoO_2, are the main phases in the temperature range between 500 and 600°C. The presence of molybdate can be corroborated by the IR spectra of the samples heated at 550 and 600°C which show bands in the 1000 cm^{-1} region assigned to the Mo(VI)–O stretching and Mo–O terminal bonds [27–29]. They disappear at a higher temperature. So, the IR spectra of the samples heated above 600°C and up to 900°C show a broad band below 700 cm^{-1} (700–300 cm^{-1}) typical of the V(III)–O, Al(III)–O and Mo(IV)–O bonds. Finally, the IR spectrum of the sample heated up to 1050°C is similar to that observed for M_2O_3 phases [30].

It is also interesting to note that the solid state chemistry of aluminum is very complex and amorphous, or "transition aluminas", are formed during heating, depending on experimental conditions [31]. All these phases are transformed into the stable

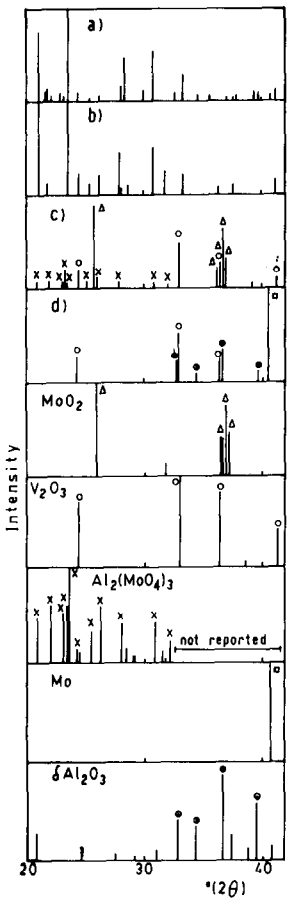

Fig. 3. Comparison of the XRD patterns of: a, $AlVMoO_7$ without thermal treatment; b, c, and d, correspond to samples heated at 500, 600 and 1000°C respectively. Additional patterns are included for reference.

rombohedral α-Al_2O_3 at a temperature higher than 1000°C. From the XRD data it is possible to suggest that Al is partially incorporated in both MoO_2 and V-oxides. A slight shift of the lines to higher 2θ angles corresponds to the $(V_{1-x}Al_x)_2O_3$ solid solution, which belongs to the corundum structure [32]. It stabilizes the presence of Al in this type of lattice at a low temperature. The remaining Al(III), incorporated in MoO_2, segregates to δ-Al_2O_3 when the reduction from Mo(IV) to Mo^0 takes place at $T = 955$°C. This phase is slowly transformed into α-Al_2O_3 by further heating. In Fig. 3d, the most intense δ-Al_2O_3 lines are detected, while all the lines of the $(V_{1-x}Al_x)_2O_3$ phase remain unchanged. A new diffraction line corresponding to the 110 plane of the metallic Mo^0 is also observed.

Finally, scanning electron microscopy reveals the morphological alterations produced during the different steps of the thermal reduction (Fig. 4). From the EPMA metallic data, given in Table 1 and the corresponding micrographs of the figure, it is

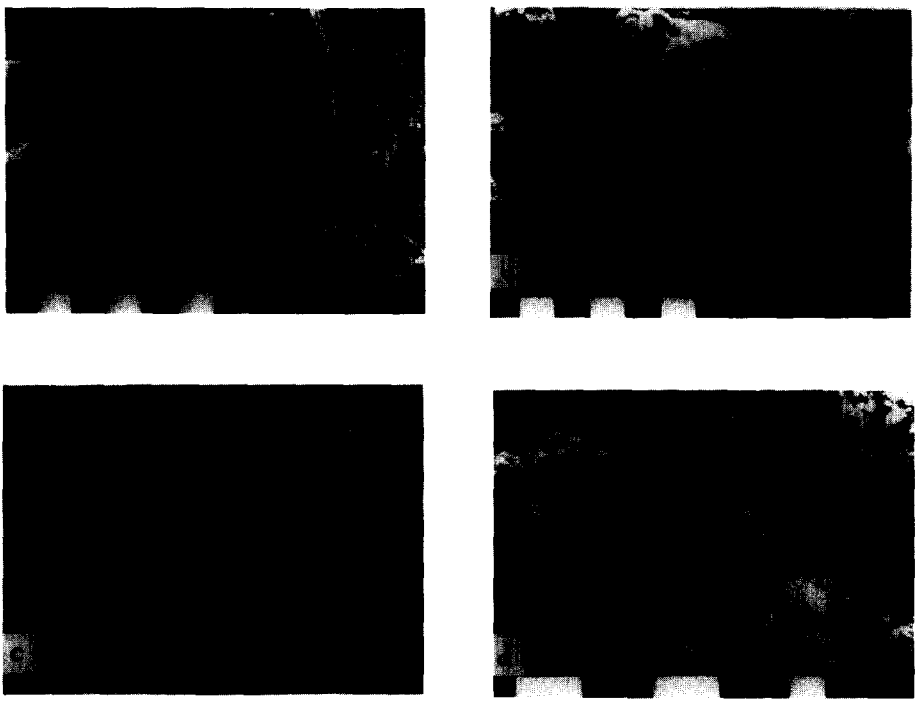

Fig. 4. Comparative scanning electron micrographs of $AlVMoO_7$: a, $AlVMoO_7$ (magnification × 1000, scale bar = 10 μm); b, TPR 500°C (magnification × 1000, scale bar = 10 μm); c, TPR 600°C (magnification × 2000, scale bar-10 μm); d, TPR 1000°C (magnification × 2000, scale bar = 10 μm).

Table 1
EPMA of the analyzed samples

Sample	% Al	% V	% Mo
$AlVMoO_7$	15.50	29.30	55.18
TPR 500°C	6.28	27.20	66.50
TPR 600°C	14.14	27.02	58.83
TPR 1000°C	3.60	19.60	76.88

possible to analyze the chemical composition of the surface. The comparative micrographs in Fig. 4b and c suggest the formation of a complex mixture poorly crystalline at 500°C. The presence of unreacted $AlVMoO_7$, from XRD data, suggests a partial decomposition to $Al_2(MoO_4)_3$, VO_x ($X \approx 2$), MoO_x ($X < 3$) and Al_2O_3, according to stoichiometric ratio. From the EPMA analysis, it can be suggested that a partial growing of aluminum molybdate, which crystallizes as a primary phase, as well as of amorphous vanadium and molybdenum oxides on the surface of the $AlVMoO_7$,follow

Table 2
Products from the different stages of thermal reduction

Temperature/°C	Phase composition of the sample
500	$VO_{X\approx 2}$, $AlVMoO_7$, $Al_2(MoO_4)_3$, Al_2O_3, MoO_X ($X < 3$)
600	MoO_2 [a], V_2O_3 [a]
1050	Mo, V_2O_3 [a], δ-Al_2O_3

[a] With Al incorporated.

a shrinking core model. However, the decrease in the aluminum content suggest that the nucleus of amorphous Al_2O_3 has not reached the size of the remaining products and is covered by them. Above 600°C, the $Al_2(MoO_4)_3$ phase reduces to "MoO_2" and "Al_2O_3" oxides, which in the presence of V(III) form the interstitial $(Mo,Al)O_2$ and the substitutional $(V_{1-x}Al_x)_2O_3$ new phases. A uniform presence of Al(III) corroborates this assumption in Fig. 4c, where the Al, Mo and V-EPMA values are similar to that observed in the original sample. However, the small differences suggest the presence of a higher proportion of $(Mo,Al)O_2$ on the surface. This situation remains practically unchanged up to 955°C, when the instertitial phase is reduced to Mo^0. The tetragonal δ-Al_2O_3 phase is then segregated. The Mo proportion increases considerably whereas the Al value decreases appreciably. This can be explained by the presence of tiny crystals of metallic Mo which are located fundamentally on the surface of the δ-variety of alumina as well as on the corundum solid solution. Crystals of δ-Al_2O_3 and rhombohedral $(V_{1-x}Al_x)_2O_3$ are observed on the left of the micrograph Fig. 4d.

The phases present in the different steps of the thermal reduction of the $AlVMoO_7$ are detailed in Table 2.

4. Conclusions

The formation of the $(V_{1-x}Al_x)_2O_3$ solid solution is observed from $\approx$600°C until the highest possible temperature is reached. The intermediate $Al_2(MoO_4)_3$ phase is observed between 500 and 600°C. The incorporation of Al in the MoO_2 monoclinic lattice, obtained by decomposition of aluminum molybdate, delays the reduction reaction to the metallic Mo. During this process, which occurs approximately 100°C above the pure MoO_2, the aluminum segregates as δ-Al_2O_3, changing to the α-phase by further heating.

Acknowledgements

This work was supported by CONICET (Programa QUINOR) and CICPBA. The authors are indebted to Mr. Fernando Ivorra (CINDECA) for the TPR measurements.

References

[1] J. Walczak, M. Kurzawa and E. Filipek, J. Therm. Anal., 31 (1986) 271.
[2] J. Walczak and M. Kurzawa, J. Therm. Anal., 31 (1986) 531.
[3] J. Walczak and E. Filipek, Thermochim. Acta, 150 (1989) 125.
[4] J. Walczak and P. Tabero, J. Therm. Anal., 36 (1990) 2173.
[5] M. Kurzawa, J. Mater. Sci. Lett., 11 (1992) 976.
[6] J. Walczak, E. Filipek and E. Tabero, Thermochim. Acta, 206 (1992) 279.
[7] F. Trifiro, V. De Vecchi and I. Pasquon, J. Catal., 15 (1969) 17.
[8] F. Trifiro, P. Forzatti and P.L. Villa, in B. Delmond, P. Jacobs and G. Poncelet (Eds.), Preparation of Catalysts, Elsevier, Amsterdam, 1976, p.147.
[9] D. Klissurski and R. Dimitrova, Bull. Chem. Soc. Jpn., 63 (1990) 590.
[10] A. Jones and B. McNicol, Temperature Programmed Reduction for Solid Materials Characterization, Marcel Dekker Inc., New York, 1986.
[11] M.B. Vassallo and I.L. Botto, Thermochim. Acta, 220 (1993) 277.
[12] M.B. Vassallo, I.L. Botto and R. Saez Puche, to be published.
[13] R. Thomas, E.M. Van Oers, V.H.J. De Beer, J. Medema and J.A. Moulijn, J. Catal., 76 (1982) 241.
[14] P.E. Werner, Ark. Kemi, 31 (1969) 513.
[15] H.C. Yao, J. Catal., 70 (1981) 440.
[16] F.J.J.G. Janssen, J. Therm. Anal., 37 (1991) 1281.
[17] C.I. Cabello, I.L. Botto and H.J. Thomas, Thermochim. Acta, 232 (1994) 183.
[18] I.L. Botto, C.I. Cabello and H.J.Thomas, Thermochim. Acta, 211 (1992) 229.
[19] J. Brito and J. Laine, Polyhedron, 5 (1986) 179.
[20] A. Baiker and D. Monti, J. Catal., 91 (1985) 361.
[21] R.A. Koeppel, J. Nickl and A. Baiker, Catal. Today, 20 (1994) 45.
[22] W.K. Hall and F.E. Massoth, J. Catal., 34 (1974) 41.
[23] R.D. Shannon, Acta Crystallogr. Sect. A, 32 (1976) 751.
[24] B.O. Marinder and A. Magneli, Acta Chem. Scand., 11 (1957) 1635.
[25] B.G. Hyde and S. Andersson, Inorganic Crystal Structures, J. Wiley and Sons, New York, 1989, p. 98.
[26] N.J. Stedman, A. K. Cheetham and P.D. Battle, J. Mater. Chem., 4 (1994) 641.
[27] E. Payen, S. Kasztelan, J. Grimblot and J.P. Bonnelle, J. Raman Spectrosc., 17 (1986) 233.
[28] P. Forzatti, C.M. Mari and P. Villa, Mater. Res. Bull., 22 (1987) 1597.
[29] P.A. Spevack and N.S. McIntyre, J. Phys. Chem., 96 (1992) 9029.
[30] S.D. Ross, Inorganic IR and Raman Spectra, Mc Graw Hill, London, 1972.
[31] F. Abbattista, S. Delmastro, G. Gozzelino, D. Mazza, M. Vallino, G. Busca, V. Lorenzelli and G. Ramis, J. Catal., 117 (1989) 42.
[32] V.V. Viktorov, Phys. Status Solidi b, 179 (1993) 531.